

## Supporting Information

# Constructing asymmetric active sites on defective Ru/W<sub>18</sub>O<sub>49</sub> for photocatalytic nitrogen fixation

Huan Shang,<sup>ac</sup> Yongjie Wang,<sup>b</sup> Hongbao Jia,<sup>a</sup> Minghan Qu,<sup>a</sup> Xingyu Ye,<sup>b</sup> Qiong Zhu,<sup>b</sup> Dieqing Zhang,<sup>c</sup>

Ding Wang,<sup>a</sup> Guisheng Li,<sup>\*ab</sup> and Hexing Li<sup>\*c</sup>

<sup>a</sup>School of Materials and Chemistry, University of Shanghai for Science and Technology, Shanghai, 200093, P. R. China

<sup>b</sup>School of Environmental and Geographical Sciences, Shanghai Normal University, Shanghai, 200234, P. R. China

<sup>c</sup>The Education Ministry Key Lab of Resource Chemistry, Joint International Research Laboratory of Resource Chemistry of Ministry of Education, Shanghai Key Laboratory of Rare Earth Functional Materials, and Shanghai Frontiers Science Center of Biomimetic Catalysis, Shanghai Normal University, Shanghai 200234, P. R. China.

\*Corresponding author. Phone/fax: +86-21-55271726

Email address: hexing-li@shnu.edu.cn; liguisheng@shnu.edu.cn

**10 pages, 9 figures, 1 table**

## CONTENTS

<b>Figure S1.</b> Plots of $(ah\nu)^{1/2}$	S5
<b>Figure S2.</b> BET	S5
<b>Figure S3.</b> EPR	S6
<b>Figure S4.</b> Photocatalytic ammonia production in the cyclic tests	S6
<b>Figure S5.</b> XRD patterns	S7
<b>Figure S6.</b> Room-temperature steady-state PL spectra	S7
<b>Figure S7.</b> N <sub>2</sub> -TPD profiles	S8
<b>Figure S8.</b> TEM	S8
<b>Figure S9.</b> Control experiment of Ru/SiO <sub>2</sub>	S9
<b>Table S1.</b> BET results	S10

## 1. Characterization

X-ray diffraction (XRD) patterns were recorded with a Rigaku Dmax-3C operated at 40 kV and 30 mA. Transmission electron microscopy (TEM) images and high-resolution transmission electron microscopy (HRTEM) were obtained on the JEOL-2010FEF at 200 kV. Electron paramagnetic resonance (EPR) spectra were recorded on an EMX PLUS spectrometer (Bruker). X-ray photoelectron spectroscopy (XPS) data were obtained on Perkin-Elmer PHI 5000. UV/Vis Diffuse Reflectance Spectra (DRS) were measured using a MC-2530 instrument spectrometer. Raman spectra were obtained by a confocal microprobe spectrometer (Thermo DXR Microscope). Fourier transform infrared spectroscopy (FTIR) spectra were performed using a Nicolet iS10 spectrometer. Photoelectrochemical measurements were performed on CHI660E workstation using three-electrode cell with a photocatalyst samples as working electrode, a Pt foil as counter electrode and a standard Ag/AgCl reference electrode, respectively. The N<sub>2</sub> adsorption performances were characterized by a temperature-programmed desorption instrument (TPD, TriStar II 3020). Photoluminescence (PL) spectra were performed on FLS1000 fluorescence spectrophotometer (Edinburgh Instruments).

## 2. Photocatalytic nitrogen fixation

The photocatalytic N<sub>2</sub> reduction experiments were performed at ambient conditions. Typically, 0.02g of catalyst was added into 80 mL deionized water. After the formation of a uniform catalyst suspension by ultrasonic treatment, the high-purity nitrogen was bubbled through the suspension to obtain a N<sub>2</sub>-saturated environment. A Xe lamp (300 W) was used as simulated solar light source, and the light source was turned on to start the reaction. Conditions: nitrogen was injected into the reaction system at a flow rate of 10 mL/min. The overall reaction time was 4 h, and samples were taken in 1 h. The

concentrations of  $\text{NH}_4^+$  were determined by Nessler's reagent method. The quantification of hydrazine ( $\text{N}_2\text{H}_4$ ) was measured by the method of Watt and Chrisp.

### 3. Supplementary figures and text

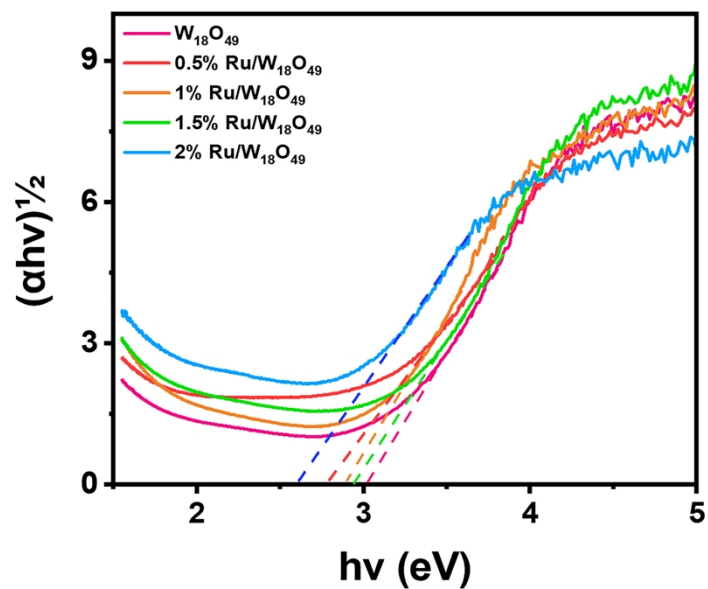


Figure S1. Plots of  $(\alpha hv)^{1/2}$  versus photon energy for calculation of bandgap.

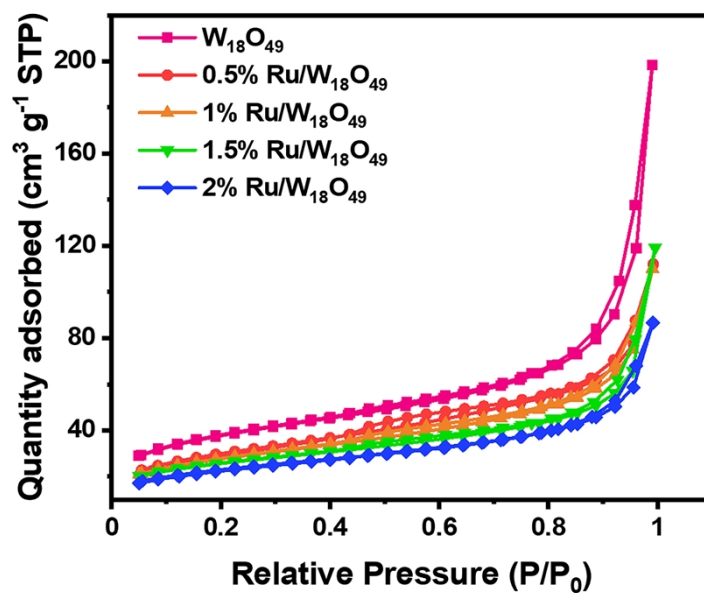
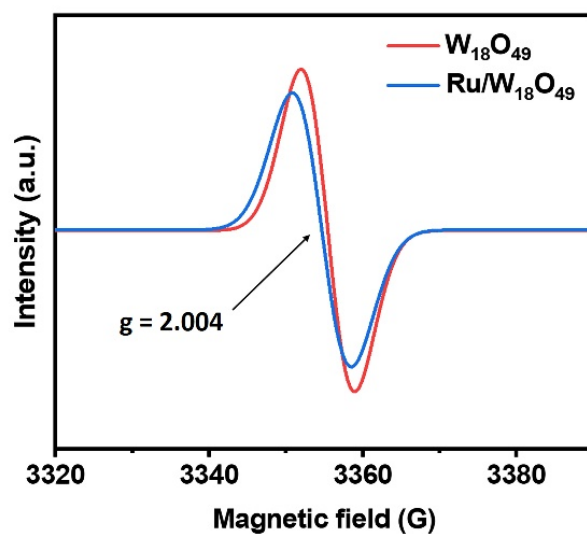
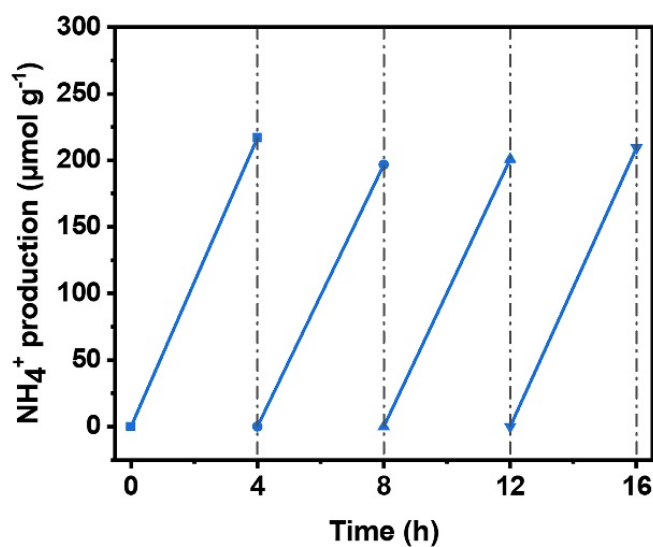


Figure S2. BET of prepared samples.



**Figure S3.** EPR spectra of  $W_{18}O_{49}$  and 1.5 %  $Ru/W_{18}O_{49}$  at 150 K.



**Figure S4.** Photocatalytic ammonia production in the cyclic tests of  $Ru/W_{18}O_{49}$ .

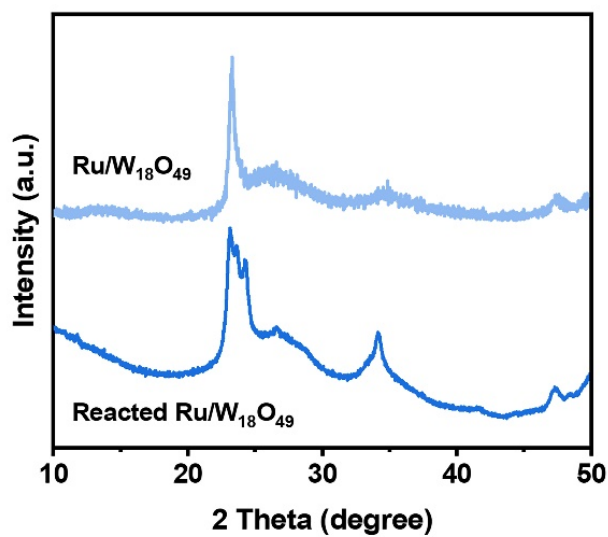


**Figure S5.** XRD patterns of Ru/W<sub>18</sub>O<sub>49</sub> and reacted Ru/W<sub>18</sub>O<sub>49</sub>.

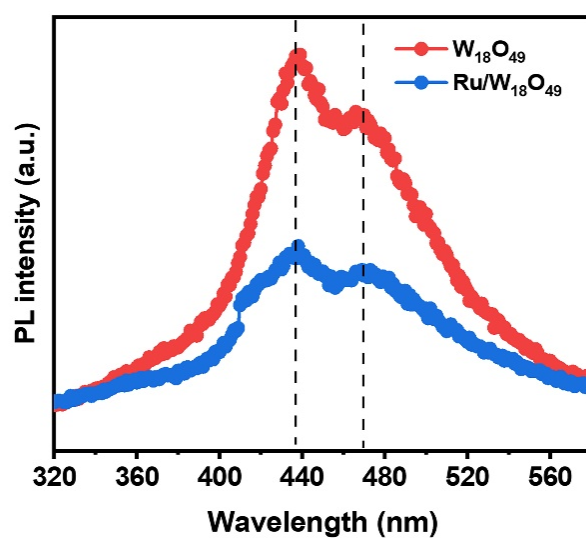


**Figure S6.** Room-temperature steady-state PL spectra of W<sub>18</sub>O<sub>49</sub> and Ru/W<sub>18</sub>O<sub>49</sub> with an excitation light of 300 nm.

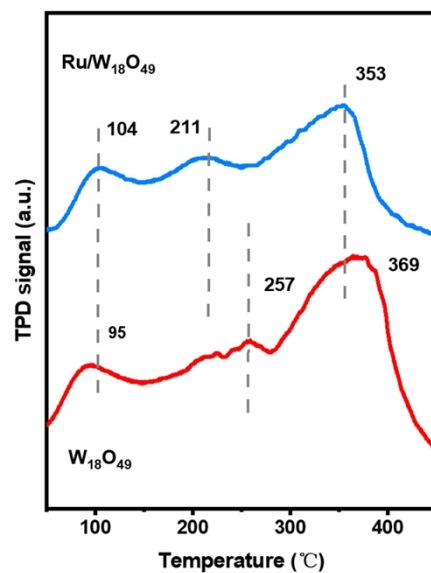


**Figure S7.** N<sub>2</sub>-TPD profiles of W<sub>18</sub>O<sub>49</sub> and Ru/W<sub>18</sub>O<sub>49</sub>.

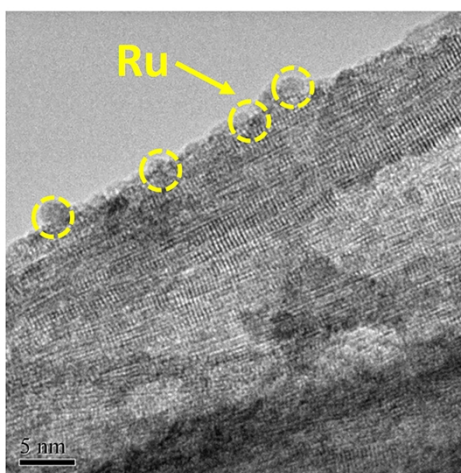


**Figure S8.** TEM image of 1.5% Ru/WO<sub>3</sub>.



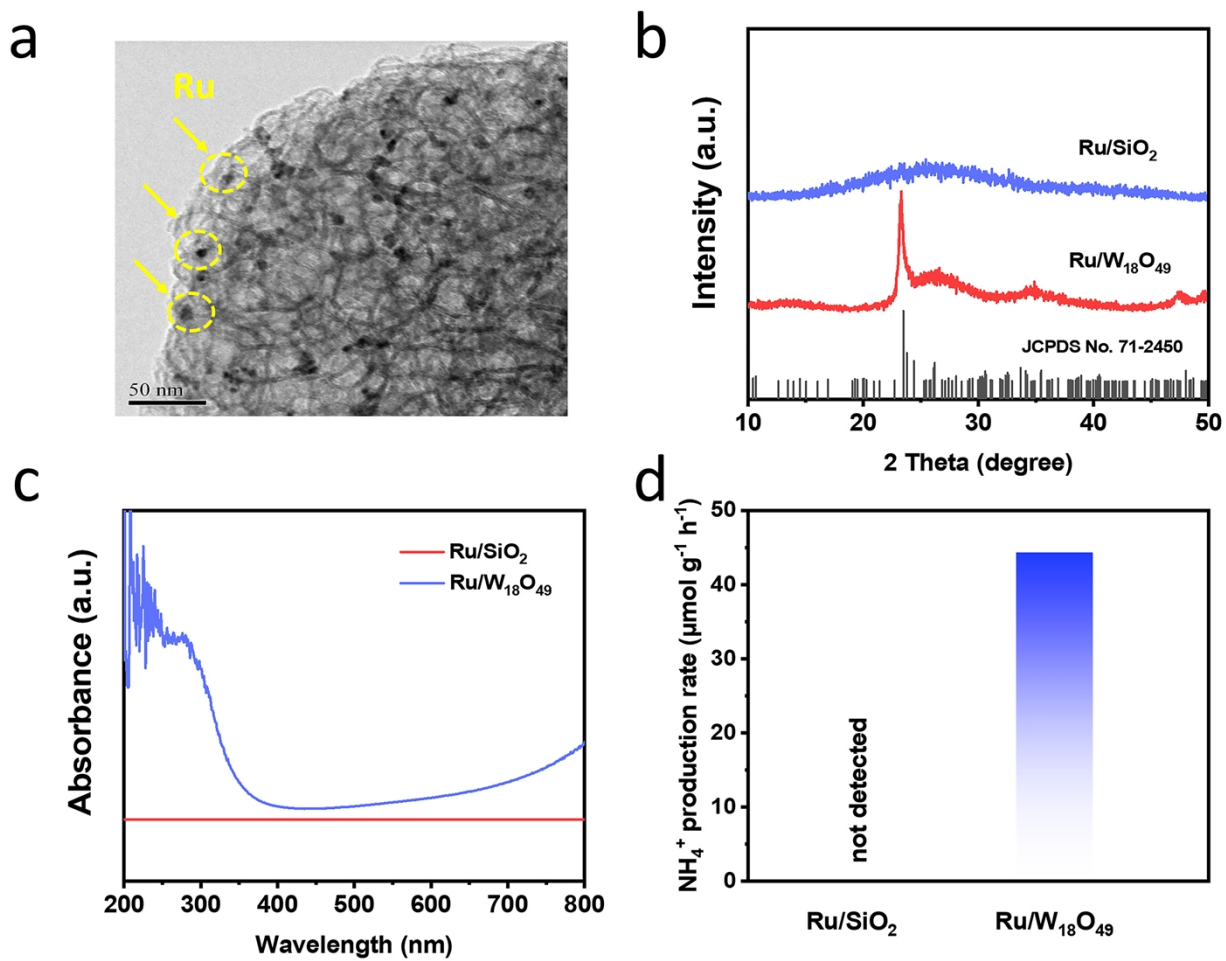


**Figure S9.** (a) TEM image. (b) XRD patterns. (c) UV/Vis absorption spectra. (d) Photocatalytic ammonia production rate on Ru/SiO<sub>2</sub> (1.5%) and Ru/W<sub>18</sub>O<sub>49</sub> (1.5%).

**Table S1** BET of samples

<b>Samples</b>	<b>BET (m<sup>2</sup>/g)</b>
<b>W<sub>18</sub>O<sub>49</sub></b>	<b>129.8</b>
<b>0.5% Ru/W<sub>18</sub>O<sub>49</sub></b>	<b>104.3</b>
<b>1.0% Ru/W<sub>18</sub>O<sub>49</sub></b>	<b>95.9</b>
<b>1.5% Ru/W<sub>18</sub>O<sub>49</sub></b>	<b>87.4</b>
<b>2% Ru/W<sub>18</sub>O<sub>49</sub></b>	<b>84.7</b>